CHIN. PHYS. LETT. Vol. 34, No. 7 (2017) 076101

Recrystallization Phase in He-Implanted 6H-SiC *

Yu-Zhu Liu(刘玉柱)[1], Bing-Sheng Li(李炳生)[2**], Hua Lin(林华)[1], Li Zhang(张莉)[3]

[1]*Jiangsu Collaborative Innovation Center on Atmospheric Environment and Equipment Technology, Nanjing University of Information Science & Technology, Nanjing 210044*

[2]*Institute of Modern Physics, Chinese Academy of Sciences, Lanzhou 730000*

[3]*Department of Physics, School of Science, Lanzhou University of Technology, Lanzhou 730050*

(Received 1 April 2017)

The evolution of the recrystallization phase in amorphous 6H-SiC formed by He implantation followed by thermal annealing is investigated. Microstructures of recrystallized layers in 15 keV He^+ ion implanted 6H-SiC (0001) wafers are characterized by means of cross-sectional transmission electron microscopy (XTEM) and high-resolution TEM. Epitaxial recrystallization of buried amorphous layers is observed at an annealing temperature of 900°C. The recrystallization region contains a 3C-SiC structure and a 6H-SiC structure with different crystalline orientations. A high density of lattice defects is observed at the interface of different phases and in the periphery of He bubbles. With increasing annealing to 1000°C, 3C-SiC and columnar epitaxial growth 6H-SiC become unstable, instead of [0001] orientated 6H-SiC. In addition, the density of lattice defects increases slightly with increasing annealing. The possible mechanisms for explanation are also discussed.

PACS: 61.80.Jh, 61.82.Fk, 68.37.Lp, 81.40.Wx DOI: 10.1088/0256-307X/34/7/076101

SiC, which has many advanced properties, is an important semiconductor material in high-speed communication and high-power control devices.[1,2] To fulfill SiC microelectronics devices, ion-implantation is the usual way to dope impurities, such as Al or P implantation. In addition, it has been shown that He implantation-induced cavities have many applications,[3–6] such as trapping metal impurities, trapping self-interstitials to inhibit the transient enhanced diffusion, ion-cut via smart-cut technology. With the development of semiconductor technology, devices become smaller and smaller, and therefore, low energy implantation is well suited for the application of semiconductor technologies. However, radiation damage generated by energetic ion implantation is a general phenomenon. Especially, SiC can be easily amorphous after ion implantation to about 0.3 displacements per atom (dpa) at room temperature (RT).[7] These lattice disorders can be removed and amorphous SiC can be recrystallized after thermal annealing. Recrystallization of amorphous SiC upon thermal annealing has been widely reported.[8–13] Recently, we have reported the amorphous layer formed in He-implanted 6H-SiC with 0.6–4 dpa at RT.[8] The threshold temperature for recrystallization is between 800℃ and 900℃. After 900℃ annealing, the recrystallized layer contains 3C-SiC and 6H-SiC with different crystalline orientations. In detail, epitaxial 6H-SiC is aligned with the underlying substrate and columnar growth 6H-SiC is formed above the 6H-SiC epitaxial layer, with the angle between the c-axes of the epitaxial 6H-SiC and columnar growth 6H-SiC of 72°. No other crystalline orientations were observed. In contrast, Bae *et al.*[9] used Xe ion implantation into 6H-SiC with $1 \times 10^{15}\,\mathrm{cm}^{-2}$ at RT followed by annealing at 890℃, and they observed the $[1\bar{1}01]$ oriented 6H-SiC layer formed above the $[1\bar{1}00]$ oriented epitaxial 6H-SiC layer the same as the substrate. They did not observe 3C-SiC and columnar 6H-SiC structure in the recrystallized layer. The formation of 3C-SiC in amorphous 6H-SiC after recrystallization has been extensively observed and can be attributed to the kinetic preference of this growth type.[10] Heera *et al.*[10] speculated columnar growth caused by additional implanted atoms or crystalline nuclear formed during irradiation. Our recent research showed that columnar growth occurs at the maximum size of helium bubbles, which is located at a depth of the maximum helium deposition. The finding indicates that implanted atoms can impede the growth of the epitaxial 6H-SiC aligned with the underlying substrate. To fulfill continual growth of the epitaxial 6H-SiC layer, columnar growth occurs. It is reasonable to speculate that columnar growth needs the lowest energy in this case. However, it has remained elusive why 3C-SiC and columnar 6H-SiC structures can be or not be formed in amorphous 6H-SiC after recrystallization. Since these different poly-types have different electronic properties, the study on the evolution of the crystalline orientation in amorphous SiC after recrystallization is important for the microelectronic industry. In the present work, 3C-SiC and columnar epitaxial growth 6H-SiC are formed in amorphous 6H-SiC after 900℃ annealing, while [0001] oriented 6H-SiC and $[1\bar{1}00]$ oriented 6H-SiC are formed after 1000℃ annealing. The possible reasons for explanation of the observed phenomena are discussed.

In our experiment, 6H-SiC wafers oriented ⟨0001⟩

*Supported by the National Natural Science Foundation of China under Grant No 11475229, and the College Students Practice Innovative Training Program of Nanjing University of Information Science & Technology under Grant No 201610300042.

**Corresponding author. Email: b.s.li@impcas.ac.cn

© 2017 Chinese Physical Society and IOP Publishing Ltd

Si surface were implanted with He^+ with 15 keV at a fluence of 3.5×10^{16} cm^{-2} at RT. The implantation experiment was performed in the 320 kV multi-discipline research platform, at the Chinese Academy of Sciences. Post-implantation, wafers were isochronally annealing in a tube furnace at 900℃ and 1000℃ for 30 min in a vacuum ($\leq1\times10^{-3}$ Pa). The microstructural evolution of the He-implanted 6H-SiC upon annealing was investigated via TEM using a Tecnai G20 operated at 200 kV and equipped with a double tilt goniometer stage. The observed images of lattice disorders, i.e., stacking faults and dislocation loops, were identified using a HRTEM with a point-to-point resolution of 0.19 nm.

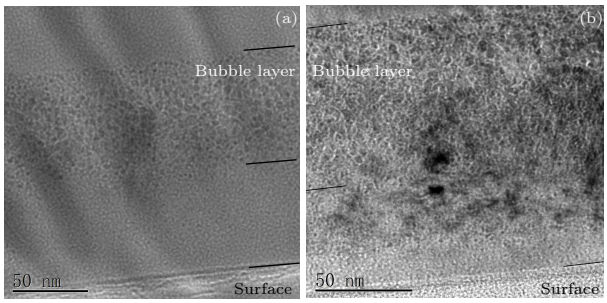

Fig. 1. Over-focus XTEM bright-field micrographs of 6H-SiC implanted with 15 keV He ions at a fluence of 3.5×10^{16} cm^{-2} at RT followed by annealing at (a) 900℃ and (b) 1000℃.

Figures 1(a) and 1(b) present a bubble layer formed beneath the surface in the He-implanted 6H-SiC after 900℃ and 1000℃ annealing, respectively. The observed bubbles exhibit a black center with white edge contrast. The mean diameter of the bubbles is 2.57 nm and the density is 2.26×10^{23} m^{-3} for the 900℃ annealed sample. After 1000℃ annealing, the mean diameter slightly increases to 2.87 nm, and the density slightly decreases to 1.95×10^{23} m^{-3}.

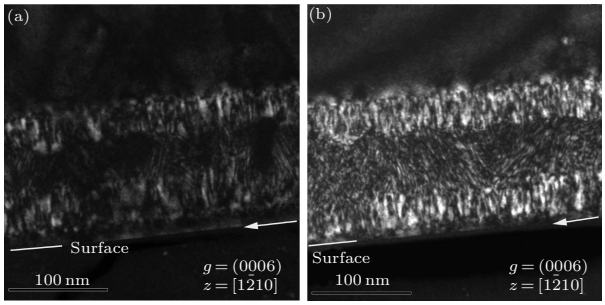

Fig. 2. XTEM two-beam dark field micrographs of the He implanted 6H-SiC after 900℃ (a) and (b) 1000℃ annealing using $\boldsymbol{g}=0006$ close to the $[1\bar{2}10]$ zone axis.

The lattice disorders of the He-implanted 6H-SiC after annealing were imaged under the two-beam dark field with $\boldsymbol{g}=0006$, and the results are shown in Fig. 2. After 900℃ annealing, there is a well damaged layer from 10 nm to 135 nm in depth, as shown in Fig. 2(a). Dense dislocation loops and stacking faults exhibiting bright contrast can be observed in the damaged layer. In the middle of the damaged layer, some zones exhibit dark contrast. HRTEM images show 3C-SiC structures in these zones. After 1000℃ annealing, the thickness of the damaged layer slightly increases to a range of surface to 145 nm in depth, as shown in Fig. 2(b). At both boundaries of the damaged layer, there are many dislocation loops inclined to the [0002] direction. In the middle of the damaged layer, many tiny dislocation loops and stacking faults can be observed. The HRTEM image shows 6H-SiC with a zone axis of [0001] formed in this zone, as shown in the following. Compared with the case of 900℃ annealing, the intensity of disorders increases significantly after 1000℃ annealing.

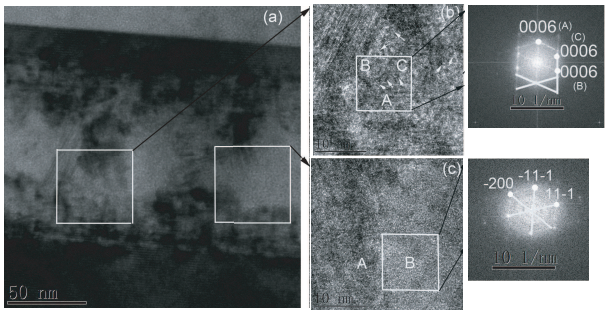

Fig. 3. (a) XTEM image showing the damaged layer of the He-implanted 6H-SiC followed by 900℃ annealing, (b) and (c) HRTEM images showing the recrystallized region in two different zones indicated by squares with Fourier-transformed patterns revealing the coexistence of A, B and C zones. Three different coexisting orientations of 6H-SiC that have the (0006) diffraction spot have been noted in the inset. Helium bubbles are indicated by arrows in Fig. 3(b).

HRTEM was performed to investigate the microstructure in the damaged layer. After 900℃ annealing, HRTEM images were taken from two zones. One zone contains two columnar 6H-SiC structures and epitaxial 6H-SiC, as shown in Fig. 3(b). The other zone contains one columnar 6H-SiC and a region that exhibited dark contrast in a dark field, as shown in Fig. 3(c). Lattice fringes can be observed in Fig. 3(b). Many He bubbles with 1–2 nm in diameter can be observed in the recrystallized layer, as indicated by arrows. Fourier transformed images taken from A–C zones in Fig. 3(b) were obtained, as shown in the insets. The pattern taken from zone A denotes that this zone is 6H-SiC with zone axis of $[1\bar{2}10]$, which has the same direction as the substrate. It is related to recrystallization and occurs at the interface of crystalline and amorphization. The patterns taken from zones B and C denote that these two zones are also 6H-SiC with a zone axis of $[1\bar{2}10]$. The angle between the c-axes of the 6H-SiC zones A and B/C is $+72°$. Likely, Fourier transformed images taken from A and B zones in Fig. 3(c) are shown in the insets. Zone A corresponds to columnar epitaxial growth 6H-SiC. The pattern taken from zone B denotes [011] oriented 3C-SiC in this zone. At first sight, the diffraction pattern seems to be close to that of 6H-SiC with a zone axis of $[1\bar{1}01]$. In that case, the angle between

$(01\bar{1}1)$ and $(\bar{1}011)$ is about 100°, and the interplanar spacing for $01\bar{1}1$ reflection is $3.8\,\mathrm{nm}^{-1}$. The experimental measurements show that the angle between the two lattice faces is 110° and interplanar spacing is $3.95\,\mathrm{nm}^{-1}$, consistent with the angle between $(\bar{1}\bar{1}1)$ and $(\bar{1}1\bar{1})$, and the interplanar spacing for $(\bar{1}1\bar{1})$ reflection of 3C-SiC. At some zones containing bubbles and an interface of A–C different zones, a mosaic of nano-sized domains can be observed. The results are due to the growth of He bubbles abided by emitting interstitial-type defects[14] as well as lattice mismatch between 3C-SiC and 6H-SiC.

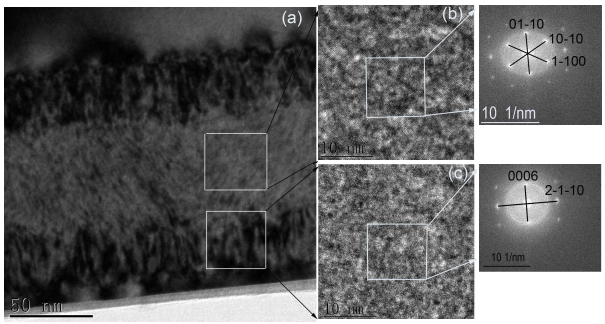

Fig. 4. (a) XTEM image showing the damaged layer of the He-implanted 6H-SiC followed by 1000℃ annealing, (b) and (c) HRTEM images showing the recrystallized region in two different zones indicated by squares with Fourier-transformed patterns revealing the coexistence of two different crystalline orientations.

After 1000℃ annealing, HRTEM images were also taken from two zones, as shown in Figs. 4(b) and 4(c). One zone is the near sample surface, where large dislocation loops were observed. The Fourier transformed pattern indicates epitaxial growth 6H-SiC with a zone axis of $[01\bar{1}0]$, as shown in the inset of Fig. 4(c). The other zone is in the middle of the damaged layer, where dense tiny dislocation loops and stacking faults were observed. The Fourier transformed pattern indicates epitaxial growth 6H-SiC with a zone axis of [0001], as shown in the inset of Fig. 4(b). Because the present experimental results show that any angle between the two lattice faces is 60° and interplanar spacings are 3.58, 3.73 and $3.67\,\mathrm{nm}^{-1}$, corresponding to $(01\bar{1}0)$, $(10\bar{1}0)$ and $(1\bar{1}00)$, respectively. The measured interplanar spacings are slightly smaller than the real ones, indicating lattice swelling on these planes.

The evolution of recrystallization phase in amorphous SiC has been extensively investigated. Heera *et al.*[10] reported that the recrystallized layer contains 3C-SiC and columnar epitaxial growth 6H-SiC during 1050℃ annealing in amorphous 6H-SiC produced by 200 keV Ge^+ ion implantation with a fluence of $1\times10^{15}\,\mathrm{cm}^{-2}$ at RT. The same reports contain 8 MeV Si^+ at a fluence of $1\times10^{16}\,\mathrm{cm}^{-2}$ implantation upon annealing at 1000℃ for 30 min,[11] 1.6 MeV He^+ at a fluence of $1\times10^{17}\,\mathrm{cm}^{-2}$ implantation upon annealing at 1500℃ for 30 min,[12] and 15 keV He^+ at a fluence of $1\times10^{17}\,\mathrm{cm}^{-2}$ implantation upon annealing at 1200℃ for 30 min.[8] However, Bae *et al.*[9] reported that the recrystallized layer only contains $[1\bar{1}00]$ and $[1\bar{1}01]$ oriented 6H-SiC during 890℃ annealing for 2 h in amorphous 6H-SiC produced by 150 keV Xe^+ with a fluence of $1\times10^{15}\,\mathrm{cm}^{-2}$ at RT. Our present experimental results show that 3C-SiC and columnar epitaxial growth 6H-SiC were formed in the recrystallized layer after 900℃ annealing, while $[1\bar{1}00]$ and [0001] oriented 6H-SiC were formed after 1000℃ annealing. According to the above experimental results, it is reasonable to regard that the formation of 3C-SiC and columnar epitaxial growth 6H-SiC is the initial stage in amorphous 6H-SiC after recrystallization. In this stage, epitaxial regrowth is not complete due to dense lattice disorders located in the interface between the columnar epitaxial growth 6H-SiC and 3C-SiC. In the second stage, continual increasing temperature or time, 3C-SiC and columnar epitaxial growth 6H-SiC turn into other oriented 6H-SiC, i.e., $[1\bar{1}01]$ and [0001]. Bae *et al.*[9] regarded impurity atoms that accumulate at the amorphous/epitaxially grown crystalline interface, leading to an unstable amorphous/epitaxially grown crystalline interface. As a result, twinned crystal occurs with a high impurity atom concentration at the interface between epitaxial and twinned crystals.

The threshold temperature for complete recrystallization of amorphous 6H-SiC formed by He implantation is 900℃. As we know, the silicon vacancy in SiC becomes mobile at 800–900℃ and helium atoms dissociate from small vacancy-type defects above 800℃.[15] The present experimental results show that the mean size of observed bubbles increases, while the density decreases with increasing the temperature. The swelling due to bubbles can be expressed as

$$S = \frac{4\pi}{3}\left(\frac{d}{2}\right)^3\rho,$$

where S, d and ρ are the swelling, the bubble diameter and the bubble density, respectively. According to the experimental result, the values of S are 0.2% and 0.24% for the He-implanted samples upon 900℃ and 1000℃ annealing, respectively, indicating helium bubbles grown via vacancy accumulation during annealing at 1000℃. Our recent research confirmed that the decrease of vacancy concentration and lack of the inner free surface of the bubbles lead to the solid phase epitaxial growth of the amorphous layer produced by He implantation.[4] Therefore, the rate of the solid phase epitaxial growth is faster at 1000℃ than that at 900℃. After 1000℃ annealing, the 3C-SiC and columnar epitaxial growth 6H-SiC become unstable, which turn into [0001] oriented 6H-SiC. One reason is that the interplant spacings of 3C-SiC are different from 6H-SiC, and therefore, the 3C-SiC structure has a high free energy compared with 6H-SiC. It is still a question why the formation of $[1\bar{1}01]$ oriented 6H-SiC in Xe-implanted 6H-SiC, but the formation of [0001] oriented 6H-SiC in He-implanted 6H-SiC.

In summary, we have investigated the recrystallization phase of 15 keV He-implanted 6H-SiC at a

fluence of $3.5 \times 10^{16}\,\mathrm{cm}^{-2}$ followed by annealing at 900℃ and 1000℃ for 30 min. XTEM and HRTEM are employed to investigate the microstructural evolution upon annealing. The sizes of helium bubbles increase, while their density decreases with increasing annealing. Lattice disorders are imaged with two-beam under $\boldsymbol{g} = 0006$, and the lattice disorder increases significantly after 1000℃ annealing. It is related to bubble growth abided by emitting interstitials and a formation of a new phase of 6H-SiC. After 900℃ annealing, the recrystallization contains 3C-SiC, columnar epitaxial growth 6H-SiC and epitaxial growth 6H-SiC the same as the underlying substrate. There are dense lattice defects located at the interface of different phases and in the periphery of helium bubbles. After 1000℃ annealing, the columnar epitaxial growth 6H-SiC and 3C-SiC disappear, instead of the [0001] orientated 6H-SiC epitaxial layer, compared with $[1\bar{1}00]$ oriented substrate. The present experimental results demonstrate that impurity atoms play an important role on amorphous SiC after recrystallization. The influence of impurity atoms on epitaxial growth is still questionable, which should be further investigated via theory simulation.

We would like to warmly thank the staff in the 320 keV high-voltage platform and the instruments and equipments sharing platform in the Institute of Modern Physics for their assistance in the ion implantation experiment. In addition, we would like to appreciate Xu Lijun for the TEM measurement.

References

[1] Choyke W J and Pernsl G 1997 *Mater. Res. Soc. Bull.* **22** 25
[2] Park C H, Cheong B H, Lee K H and Chang K J 1994 *Phys. Rev.* B **49** 4485
[3] Kazan M, Ottaviani L, Moussaed E, Nader R and Masri P 2008 *J. Appl. Phys.* **103** 053707
[4] Boninelli S, Claverie A, Impellizzeri G, Mirabella S, Priolo F, Napolitani E and Cristiano F 2006 *Appl. Phys. Lett.* **89** 171916
[5] Tong Q Y, Lee T H, Werner P, GÖsele U, Bergmann R B and Werner J H 1997 *J. Electrochem. Soc.* **144** L111
[6] Raineri V, Fallica P G and Libertio S 1996 *J. Appl. Phys.* **79** 9012
[7] Weber W J, Wang L M, Yu N and Hess N J 1998 *Mater. Sci. Eng.* A **253** 62
[8] Li B S, Du Y Y and Wang Z G 2015 *Nucl. Instrum. Methods Phys. Res. Sect.* B **345** 53
[9] Bae In-Tae, Ishimaru M, Hirotsu Y and Sickafus K E 2004 *J. Appl. Phys.* **96** 1451
[10] Heera V, Kogler R, Skorupa W and Stoemenos J 1995 *Appl. Phys. Lett.* **67** 1999
[11] Harada S, Ishimaru M, Motooka T, Nakata T, Yoneda T and Inoue M 1996 *Appl. Phys. Lett.* **69** 3534
[12] Olivero E, David M L, Beaufort M F, Nomgaudyte J, Pranevicius L, Declemy A and Barbot J F 2002 *J. Appl. Phys.* **91** 1179
[13] Liu Y Z, Li B S and Zhang L 2017 *Chin. Phys. Lett.* **34** 052801
[14] Li B S, Zhang C H, Zhang H H, Shibayama T and Yang Y T 2011 *Vacuum* **86** 452
[15] Itoh H, Hayakawa N, Nashiyama I and Sakuma E 1989 *J. Appl. Phys.* **66** 4529